Organic LETTERS

Letter

pubs.acs.org/OrgLett

Spirodalesol, an NLRP3 Inflammasome Activation Inhibitor

Ai Hua Zhang,[†,∥] Wen Liu,[†] Nan Jiang,[§] Qiang Xu,[†] and Ren Xiang Tan*[,†,‡]

[†]Institute of Functional Biomolecules, State Key Laboratory of Pharmaceutical Biotechnology, Nanjing University, Nanjing 210046, China

[‡]School of Pharmacy, Nanjing University of Chinese Medicine, Nanjing 210023, China

[§]School of Pharmacy, Nanjing Medical University, Nanjing 210029, China

[∥]State Key Laboratory of Elemento-organic Chemistry, Nankai University, Tianjin 300071, China

Supporting Information

ABSTRACT: Autoimmune and inflammatory diseases are associated with inappropriate activation of the NOD-like receptor protein 3 (NLRP3) inflammasome, but suitable inhibitors against such improper activations remain scarce. Here, spirodalesol (**1**) from *Daldinia eschscholzii* was structurally characterized and is biosynthetically proposed as an NLRP3 inflammasome activation inhibitor with an unprecedented carbon skeleton.

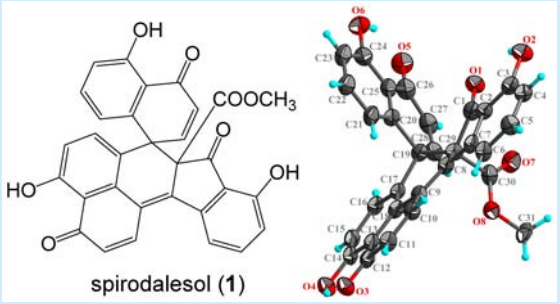

Inflammasomes, which essentially contribute to inflammation, are protein complexes capable of promoting caspase activation, leading to the processing of interleukin-1β (IL-1β) and cell death as the passive responses to infection and injury.[1] The best characterized is the NOD-like receptor protein 3 (NLRP3) inflammasome, whose inappropriate or excessive activation has been evidenced to be causative for many autoimmune and inflammatory diseases such as sepsis, diabetes, hyperuricemia, Alzheimer's disease, multiple sclerosis, and inflammatory bowel syndrome.[2] The NLRP3 inflammasome has therefore been accepted as an effective therapeutic target because inhibition of its activation may abrogate or substantially attenuate the damaging inflammation.[1a,2] However, less attention has been paid to the highly desired selectivity in targeting the different steps of inflammasome activation. There is an urgent need to exploit lead- and drug-like small molecules with unprecedented scaffolds capable of inhibiting activation of the NLRP3 inflammasome.[1a,2]

The secondary metabolites of *Daldinia eschscholzii* strains isolated from terrestrial[3,5a] and marine niches[4,5b] have been well-investigated. However, in improving the production of the immunosuppressive polyketides dalesconols A and B,[6] we found that the composition of the fermentation medium substantially affects the secondary metabolite profile of *D. eschscholzii* IFB-TL01, residing in the mantis (*Tenodera aridifolia*) gut.[3] After optimization of the nutritional parameters, the fungus was regrown on a larger scale, and the obtained extract was fractionated under the bioassay guidance to yield a skeletally undescribed and biologically active polyketide that we have named spirodalesol (**1**). In its high-resolution electrospray ionization mass spectrometry (HR-ESI-MS), spirodalesol (**1**) gave an ion at m/z 541.0897 corresponding to $[M + Na]^+$. Subsequent structure determination was accomplished by interpreting its ^{1}H and ^{13}C NMR, ^{1}H−^{1}H COSY, ROESY, HSQC, and HMBC spectra (Table S1 and Figures S7−13). The novel skeleton and relative configuration of **1** was confirmed by single-crystal X-ray diffraction, which indicated that it is a racemate with the two enantiomers signifying identically in the ^{1}H and ^{13}C NMR spectra. Subsequent chiral HPLC separation of **1** gave enantiomers (+)-**1** and (−)-**1**, which were demonstrated to have (19*S*,29*R*) and (19*R*,29*S*) configurations, respectively, by comparison of their circular dichroism (CD) spectra with those computed for all possible stereoisomers (Figure 2). Mechanistically, the first positive Cotton effect in the calculated curve, located at about 243 nm, arises from the electronic transition from the filled C=C bonding molecular orbital (MO), $\pi_{C=C}$, to the antibonding C−C orbital, σ^*_{C-C} (MO 134 → MO 139; Figure S5 and Table S3). This band could be correlated to the peak centered at 251 nm in the experimental CD curve. The next positive Cotton effect at 372 nm in the experimental CD spectrum could be correlated to the shoulder peaks at 367 and 444 nm. The electronic transitions from $\pi_{C=C}$ and the lone-pair orbital of oxygen (n_O) to the $\pi^*_{C=C}$ orbital contributed to these absorption bands (MO 128 → MO 135 and MO 133 → MO 135). In addition, the negative Cotton effects at 217, 318, and 469 nm in the experimental curves were also reproduced by the calculation at 217, 315, and 504 nm, respectively. The electronic transitions from $\pi_{C=C}$ to $\pi^*_{C=C}$ contributed to these absorption bands

Received: November 17, 2016
Published: December 7, 2016

DOI: 10.1021/acs.orglett.6b03435
Org. Lett. 2016, 18, 6496−6499

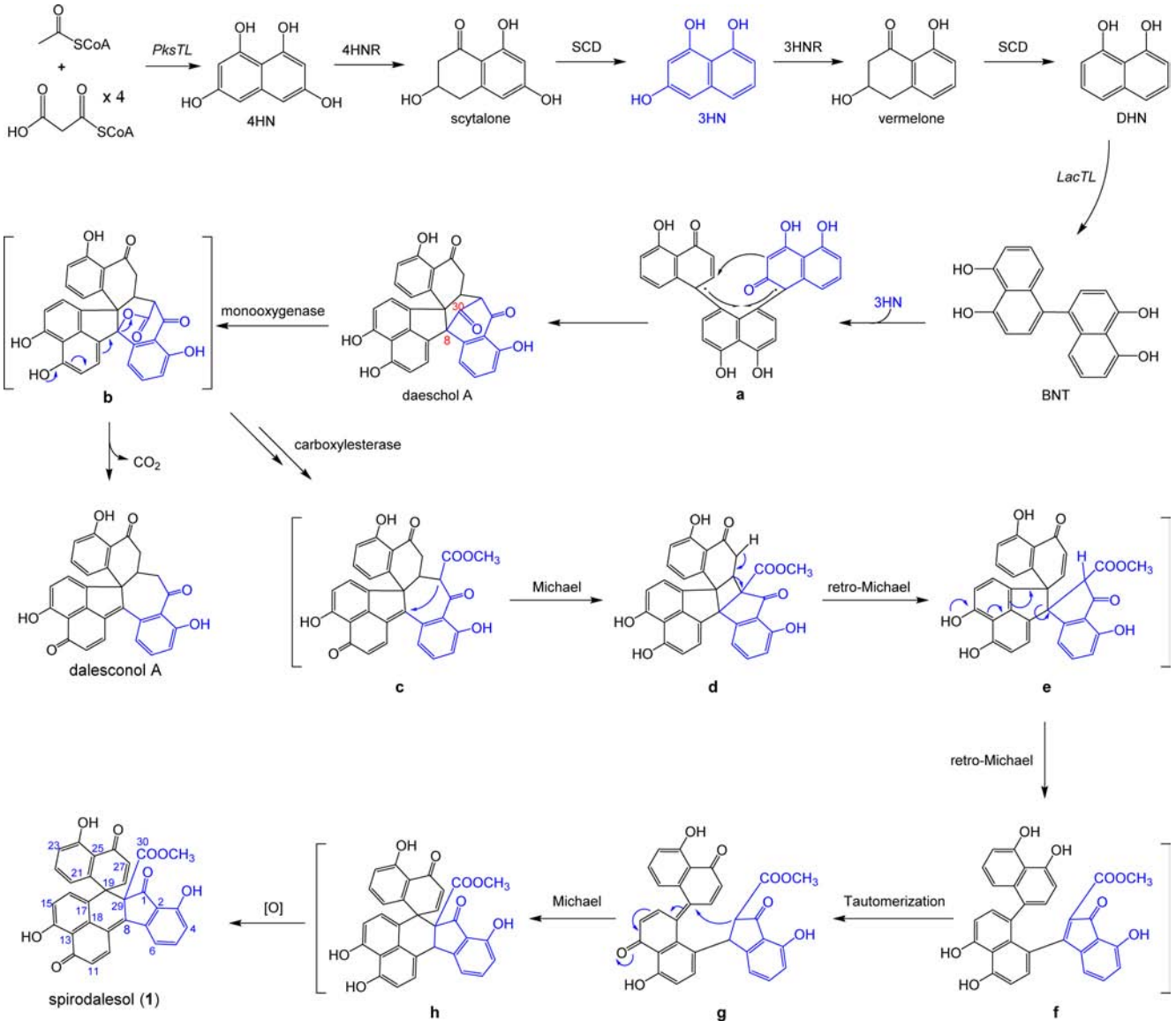

Figure 1. Plausible biosynthetic pathway of spirodalesol (**1**) as an aberrant product of dalesconol A. The two polyketides might share the early biosynthetic steps, including polyketide synthase (*pksTL*)- and laccase (*lacTL*)-catalyzed generation and coupling of 1,3,8-trihydroxynaphthalene (3HN), 1,8-dihydroxynaphthalene (DHN), and 1,1′-binaphthalene-4,4′,5,5′-tetrol (BNT).[5c] Abbreviations: 4HN, 1,3,6,8-tetrahydroxynaphthalene; 4HNR, 4HN reductase; 3HNR, 3HN reductase; SCD, scytalone dehydratase.

(MO 126 → MO 135, MO 134 → MO 135, and MO 134 → MO 142; Figure S5 and Table S3).

Structural scrutiny of **1**, daeschol A, and dalesconol A suggested that a cascade of reactions might be involved in formation of the spirodalesol architecture. Hypothetically, intermediate **c**, derived from daeschol A, might undergo an intramolecular Michael addition to produce four-membered-ring intermediate **d** (Figure 1). Two consecutive retro-Michael reactions of **d** would lead to intermediate **f**, which could be converted into **h** via tautomerization and intramolecular Michael addition reactions. Subsequent oxidation of **h** would give **1**.

With the *D. eschscholzii* genome in hand, we were able to address the biosynthetic pathway of spirodalesol (**1**). As noted with dalesconols A−C,[5c] the biosynthesis of **1** is also governed by the genes encoding polyketide synthase (*pksTL*) and laccase (*lacTL*). In fact, spirodalesol is found to be an aberrant product derived from daeschol A, a precursor of dalesconol A. In the

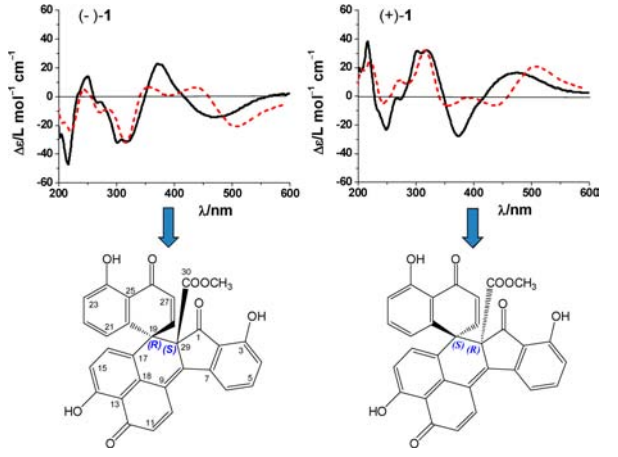

Figure 2. Absolute stereochemical assignments for (+)-**1** and (−)-**1** by comparison of the recorded (solid lines) and computed (dotted lines) ECD spectra.

DOI: 10.1021/acs.orglett.6b03435
Org. Lett. 2016, 18, 6496−6499

fungal culture, the formation of spirodalesol was found to be in parallel with the reduction of daeschol A and dalesconol A. This confirmed that spirodalesol is formed from daeschol A in competition with dalesconol A generation. This assumption was supported by the protein-catalyzed conversion of daeschol A into **1** (Figure 3), but the Michael and retro-Michael transformations were so efficient that no intermediate could be detected.

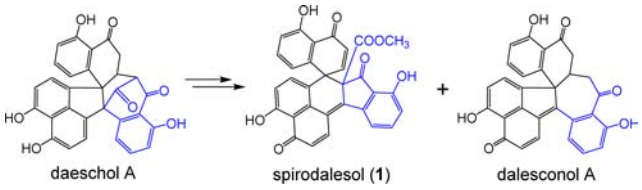

Figure 3. Intra/extracellular-protein-catalyzed transformations of daeschol A into spirodalesol and dalesconol A.

Table 1. Inhibitory Assay against IL-1β Production in THP-1 Cells with LPS+ATP-Induced NLRP3 Inflammasome Activation (IC_{50} in μM)

	compounds		
cell line	(+)-**1**	(−)-**1**	andrographolide[a]
THP-1	0.67 ± 0.11	0.7 ± 0.08	21.53 ± 0.17

[a]Coassayed as a positive control.

After the chiral resolution procedure, the spirodalesol enantiomers (+)-**1** and (−)-**1** were evaluated for their inhibitory effect on IL-1β secretion, which is indicative of NLRP3 inflammasome activation in macrophages stimulated by lipopolysaccharide (LPS) plus adenosine triphosphate (ATP).[7] As shown in Table 1, both (+)-**1** and (−)-**1** significantly suppress the secretion of IL-1β with IC_{50} values of 0.67 and 0.70 μM, respectively, which indicate approximately 30-fold greater activity than for andrographolide (IC_{50} = 21.53 μM), a prescribed drug coassayed in this study as a positive reference because of its ascertained inhibition of NLRP3 inflammasome activation.[8]

In the next experiment, we tried to address the inhibition characteristics of spirodalesol against the inflammasome activation. Interestingly, (+)-**1** showed negligible effects on TNF-α and IL-6 production (Figure 4A), suggesting selectivity in its anti-inflammatory action by downregulation of IL-1β production specifically. We therefore examined the behavior of (+)-**1** in inhibiting activation of the NLRP3 inflammasome in both bone-marrow-derived macrophage (BMDM) and mice with LPS-induced sepsis (indicative of NLRP3 inflammasome activation). The activation of caspase-1 (CASP1) was significantly inhibited by treatment with (+)-**1**, as indicated by the presence of the cleaved form in LPS plus ATP-treated BMDM cells (Figure 4B,C). NLRP3 inflammasome activation involves two signal pathways called signals I and II, which can be

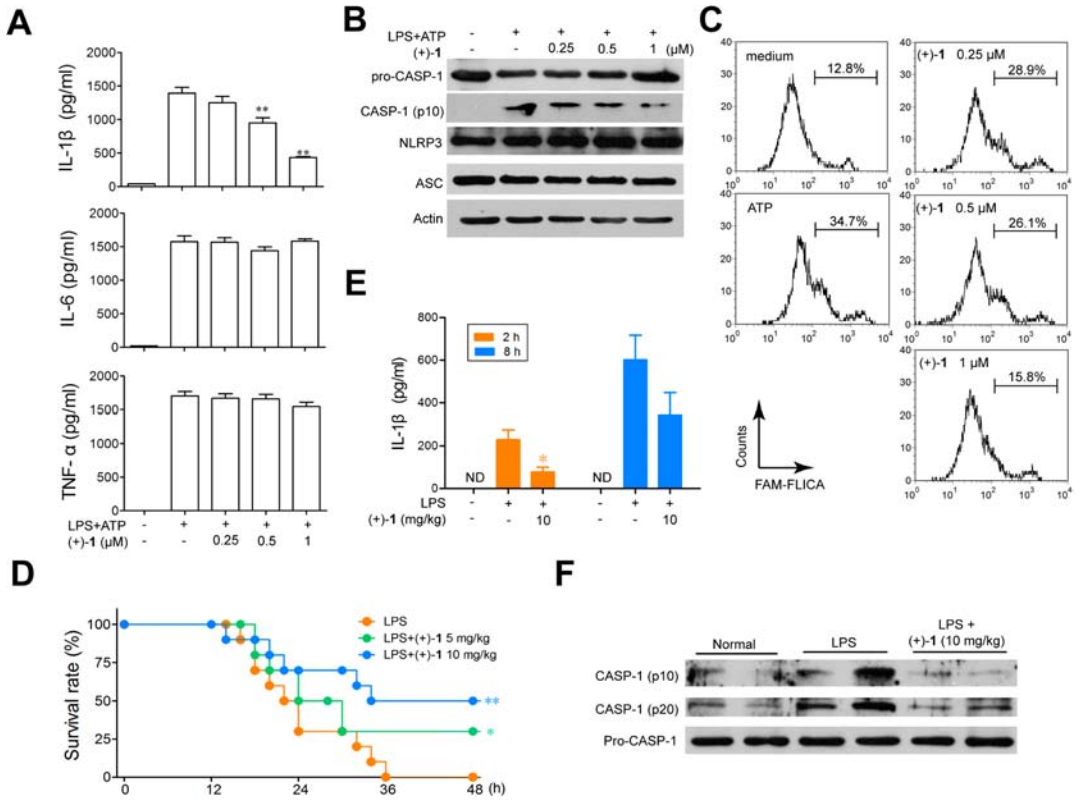

Figure 4. Effects of (+)-**1** on activation of the NLRP3 inflammasome in LPS-primed BMDM cells and in mice with LPS-induced sepsis. (A, B) LPS-primed BMDM cells were treated with the indicated doses of (+)-**1** for 1 h followed by stimulation with 5 mM ATP for another 1 h. Thereafter, the levels of IL-1β, TNF-α, and IL-6 were examined by ELISA (A) and the components of the NLRP3 inflammasome were measured by Western blot (B). Data shown are representative of three experiments. (C) BMDM cells were cultured with (+)-**1** for 1 h, followed by 1 h of incubation with 5 mM ATP. The activation of CASP-1 was determined by FAM-FLICA staining. Data shown are representative of three experiments. (D−F) Mice were treated i.g. with (+)-**1** (5 and 10 mg/kg) once a day for 3 days, followed by i.p. challenge with 10 mg/kg LPS. The survival rates were monitored continuously (D), and IL-1β in serum was measured by ELISA (E). Activation of CASP-1 in peritoneal macrophage from the mice was examined by Western blot (F). *, $P < 0.05$ vs control.

DOI: 10.1021/acs.orglett.6b03435
Org. Lett. 2016, 18, 6496−6499

triggered by LPS and ATP, respectively, to produce pro-IL-1β and CASP1.[7,9] Surprisingly, (+)-**1** selectively inhibits signal II but not signal I of inflammasome activation since it displays neither inhibition of p65 activation and luciferase activity of NF-κB nor IL-1β mRNA expression in BMDM cells (Figure S1), suggesting that its inhibition of IL-1β secretion is independent of the NF-κB signaling. This observation, along with the aforementioned results, underscores that the spirodalesol (**1**) may be valuable in the research and development of new anti-inflammatory agents.

To our knowledge, such an inhibition of the NLRP3 inflammasome assembly by (+)-**1** via interruption of the oligomerization of the ASC without affecting NF-κB signaling is authentic. It contributes to the recovery of the LPS-challenged mice, which overproduce pro-inflammatory cytokines IL-1β and TNF-α (Figures 4A and S2A), and the untreated animals died eventually of sepsis (Figure 4D). Moreover, both the IL-1β release and CASP1 activation are greatly reduced by exposure to (+)-**1**, as discerned in the peritoneal macrophage (Figure 4E,F). All of these data suggest that (+)-**1** has a unique anti-inflammatory activity against IL-1β secretion via targeting of the NLRP3 inflammasome assembly, with an IC_{50} value much lower than those of the prescribed medicines such as glyburide[10] and andrographolide.[8]

In summary, this work provides the full characterization of spirodalesol (**1**) with a unique mode of action in inhibiting NLRP3 inflammasome assembly, thereby holding promise either as a new treatment for inflammations or as a tool molecule that may find its role in the related frontier of biology and biomedicine. To our surprise, spirodalesol might be unique in the four-membered-ring-mediated skeletal rearrangement via a consortium of intramolecular Michael and retro-Michael reactions. This accommodated in turn the biosynthetic pathway, which was partially supported by enzymatic transformation experiments. Such a strategy may be of general significance in deepening the understanding of rare natural products with new chemical spaces, promising biological functions, and unforeseeable biosynthetic pathways.

■ ASSOCIATED CONTENT

Supporting Information

The Supporting Information is available free of charge on the ACS Publications website at DOI: 10.1021/acs.orglett.6b03435.

General methods, fractionation procedure, and 1D and 2D NMR spectra (PDF)

X-ray data for spirodalesol (CIF)

■ AUTHOR INFORMATION

Corresponding Author

*rxtan@nju.edu.cn

ORCID

Ren Xiang Tan: 0000-0001-6532-6261

Notes

The authors declare no competing financial interest.

■ ACKNOWLEDGMENTS

The work was successively financed by the NSFC (Grants 21672101, 81530089, 81421091, 21402090, 21661140001, and 21303086).

■ REFERENCES

(1) (a) Baldwin, A. G.; Brough, D.; Freeman, S. *J. Med. Chem.* **2016**, *59*, 1691−6710. (b) Bruno, V. M.; Shetty, A. C.; Yano, J.; Fidel, P. L., Jr; Noverr, M. C.; Peters, B. M. *mBio* **2015**, *6*, e00182-15. (c) Gross, O.; Poeck, H.; Bscheider, M.; Dostert, C.; Hannesschläger, N.; Endres, S.; Hartmann, G.; Tardivel, A.; Schweighoffer, E.; Tybulewicz, V.; Mocsai, A.; Tschopp, J.; Ruland, J. *Nature* **2009**, *459*, 433−436.

(2) Shao, B. Z.; Xu, Z. Q.; Han, B. Z.; Su, D. F.; Liu, C. *Front. Pharmacol.* **2015**, *6*, 262.

(3) Wender, P. A.; Quiroz, R. V.; Stevens, M. C. *Acc. Chem. Res.* **2015**, *48*, 752−760.

(4) Hu, Z. X.; Xue, Y. B.; Bi, X. B.; Zhang, J. W.; Luo, Z. W.; Li, X. N.; Yao, G. M.; Wang, J. P.; Zhang, Y. H. *Mar. Drugs* **2014**, *12*, 5563−5575.

(5) (a) Zhang, Y. L.; Zhang, J.; Jiang, N.; Lu, Y. H.; Wang, L.; Xu, S. H.; Wang, W.; Zhang, G. F.; Xu, Q.; Ge, H. M.; Ma, J.; Song, Y. C.; Tan, R. X. *J. Am. Chem. Soc.* **2011**, *133*, 5931−5940. (b) Tarman, K.; Palm, G. J.; Porzel, A.; Merzweiler, K.; Arnold, N.; Wessjohann, L. A.; Unterseher, M.; Lindequist, U. *Phytochem. Lett.* **2012**, *5*, 83−86. (c) Fang, W.; Ji, S.; Jiang, N.; Wang, W.; Zhao, G. Y.; Zhang, S.; Ge, H. M.; Xu, Q.; Zhang, A. H.; Zhang, Y. L.; Song, Y. C.; Zhang, J.; Tan, R. X. *Nat. Commun.* **2012**, *3*, 1039.

(6) Pan, Z. H.; Jiao, R. H.; Lu, Y. H.; Tan, R. X. *Bioresour. Technol.* **2015**, *192*, 346−353.

(7) Schroder, K.; Tschopp, J. *Cell* **2010**, *140*, 821−832.

(8) Guo, W.; Sun, Y.; Liu, W.; Wu, X.; Guo, L.; Cai, P.; Wu, X.; Wu, X.; Shen, Y.; Shu, Y.; Gu, Y.; Xu, Q. *Autophagy* **2014**, *10*, 972−985.

(9) Strowig, T.; Henao-Mejia, J.; Elinav, E.; Flavell, R. *Nature* **2012**, *481*, 278−286.

(10) Lamkanfi, M.; Mueller, J. L.; Vitari, A. C.; Misaghi, S.; Fedorova, A.; Deshayes, K.; Lee, W. P.; Hoffman, H. M.; Dixit, V. M. *J. Cell Biol.* **2009**, *187*, 61−70.

DOI: 10.1021/acs.orglett.6b03435
Org. Lett. 2016, 18, 6496−6499